Numerical Evaluation of B1-field and SAR for Heterogeneous and Homogeneous Body Model

Z. Zhai[1], G. D. DeMeester[1], M. A. Morich[1], S. M. Shvartsman[1], R. P. Kleihorst[2]

[1]Philips Medical Systems, Cleveland, Ohio, United States, [2]Philips Medical Systems, Best, Best, Netherlands

Introduction

A uniform body phantom is sought to study the electromagnetic behavior and SAR for high field systems. However, there are concerns that such a phantom cannot give results as accurate as a complex human body model with various tissues. To gain insight we use a FDTD method to numerically calculate the electric fields, magnetic fields, and SAR inside a homogeneous and a heterogeneous body model with identical external geometry at 128MHz/3T. Simulation suggests that a homogeneous phantom globally predicts electric and magnetic field distributions, but it may overestimate the whole body SAR and underestimate the local SAR in some regions.

Methods

A shielded 16-element band-pass quadrature body coil (QBC) with a mean diameter of 60cm and length of 40cm was modeled for whole body MRI at 3T. We used the XFDTD software package (Remcom, Inc., State College, PA) to model the QBC with an isotropic resolution of 5mm [1]. Copper strips and rods in the QBC were modeled as conductors with conductivity $\sigma = 5.8\times10^{7}$S/m. Capacitors in the coil rungs and end rings were modeled by assigning passive loads in the gaps opened at their locations. Tunable distributed capacitors in the coil rungs were modeled directly with conducting and dielectric materials. The body coil was fed in quadrature by assigned sinusoidal voltage sources (f =128MHz) consistent with the birdcage theory [2]. An RF shield was included with the diameter of 68cm and length of 100cm. The heterogeneous human body model with 23 district types of tissues was obtained from Remcom, Inc. Portions of the arms in the original model were removed to eliminate contacts between hands and the torso. A homogeneous human body model with the identical external geometry to the Remcom model was generated for comparison. We did this by assigning all tissue properties to the mean values for conductivity and permittivity, where the mean values are determined by a weighted average method of all tissue types. Both the heterogeneous and homogeneous body models were placed inside the QBC at the same imaging position. Steady-state solutions were recorded in each case and B_1-field in the laboratory frame was converted to the B_1^+-field in the rotating frame using the formula in Ref [2]. SAR was calculated with respect to a fixed average B_1^+-field over the central slice for both human body models.

Results

In Fig. 1, we show the diagram of a 3T QBC with a human body model (RF shield is not shown), where the abdomen is centered at the isocenter of the QBC. In Fig. 2, we show the normalized B_1^+-field ($|B_1^+|/|B_1^+|_{ave}$) in the central transverse and sagittal slices of the heterogeneous and homogeneous body models, respectively. The $|B_1^+|_{ave}$ is the average $|B_1^+|$-field over the central transverse slice as shown in Fig. 1(b) excluding the arms. Referring to Fig. 2(a) and (b), it is seen that for the particular body position modeled, the B_1^+-field in the heterogeneous body model and homogeneous body model globally have similar field patterns. The same is true for B_1^+-field in the central sagittal slice (see Fig. 2(c) and (d)) and the central coronal slice (not shown). The initially uniform B_1^+-field in the unloaded QBC is altered by the combined effects of tissue dielectric and eddy current. High dielectric constant tends to enhance the B_1^+-field in the center, while the conducting tissue tends to reduce B_1^+-field in the center and increase B_1^+-field near the peripheral regions. One does see, however, some local differences between the two models (e.g., in the sagittal plane near the anterior region). This is due to the individual tissues with different physical properties, which modify B_1^+-field locally. We notice that there is a weak B_1^+-field near the posterior region in the transverse slice because of the reversal B_1^+-field polarization [4].

In Fig 3, we show the calculated SAR in the same transverse and sagittal slices. There is some (global) similarity but local tissue conductivity has a significant effect on SAR. In Table 1, we list the calculated SAR for 1.55% duty cycle with average B_1^+-field strength over the central transverse slice $|B_1^+|_{ave}$ = 13.5μT. It is seen that, SAR values are different for the heterogeneous and homogeneous models. For the particular body position modeled at 3T, the following observations are made: (i) Maximum local SAR would exceed IEC's SAR limits [5] first, then whole body or partial body SAR, for both body models; (ii) The whole body SAR and partial body SAR of the homogeneous model are ~38% higher than those of the heterogeneous model; (iii) The homogeneous body model has 65% higher maximum local SAR in the extremities than that of heterogeneous model; (iv) The homogeneous model has 38% less maximum local SAR in the trunk than that of heterogeneous model.

Conclusions

The global similarity of E-field (not shown) and B_1^+-field patterns from the two human body models suggests that a homogeneous phantom with physical geometry that mimics the shape of a human body can be used to study global electromagnetic behavior. However, for SAR calculations, a homogeneous human body model tends to overestimate the whole body SAR and underestimate the local SAR in the trunk. Knowing this in advance can be informative for possible measurements using more complex phantom shapes.

References

[1]. Christopher M. Collins, et. al, MRM 40:847-856 (1998); T. S. Ibrahim, et. al, Magn. Reson. Imag. 18: 835-843 (2000).
[2]. J. Tropp, J. Magn. Reson. 82: 51-62 (1989).
[3]. D. I. Hoult, Concepts Magn. Reson. 12(4): 173-187 (2000).
[4]. Jinghua Wang, et, al, MRM 48: 362-369 (2002).
[5]. International Electrotechnical Commission IEC 60601-2-33.

1.55% duty cycle at $\|B_1^+\|_{ave}$ = 13.5μT	**Heterogeneous Model**	**Homogeneous Model**
Whole Body SAR (W/kg)	0.8	1.1
Partial Body SAR (W/kg)	1.5	2.1
Max. Local SAR in Extremities (W/kg)	13.1	21.6
Max. Local SAR in Trunk (W/kg)	10	6.2

Table 1. Calculated SAR for the heterogeneous and homogeneous body models with abdomen centered in a 3T QBC.

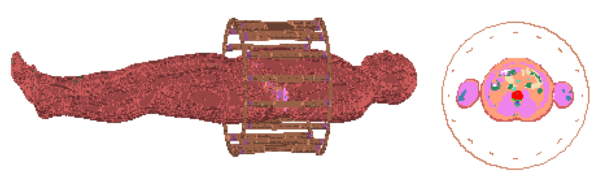

(a) (b)

Fig 1. (a) Diagram of a human body model inside a 3T QBC (RF shield is not shown); (b) Central transverse slice of the body model.

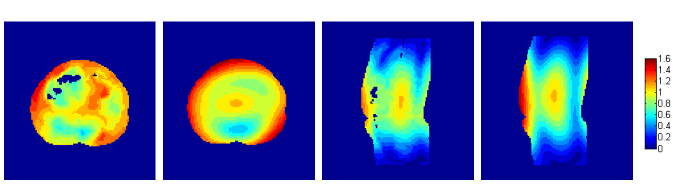

(a) (b) (c) (d)

Fig 2. $|B_1^+|$-field distribution in transverse (a, b) and sagittal (c, d) slices for heterogeneous model (a, c) and homogeneous model (b, d).

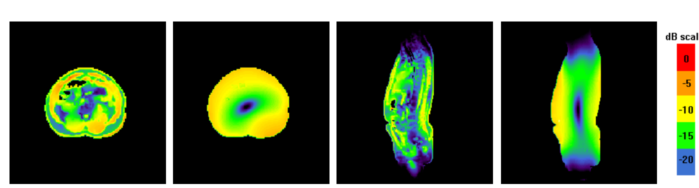

(a) (b) (c) (d)

Fig 3. SAR distribution in transverse (a, b) and sagittal (c, d) slices for heterogeneous model (a, c) and homogeneous model (b, d).